



Published in final edited form as:

*J Thorac Oncol.* 2014 July ; 9(7): 998–1007. doi:10.1097/JTO.0000000000000202.

## Frequent co-amplification and co-operation between *C-MYC* and *PVT1* oncogenes promote malignant pleural mesothelioma

Erick Riquelme, PhD<sup>1</sup>, Milind B. Suraokar, PhD<sup>1</sup>, Jaime Rodriguez, MD<sup>1</sup>, Barbara Mino, BS<sup>1</sup>, Heather Y. Lin, PhD<sup>3</sup>, David C. Rice, MD<sup>4</sup>, Anne Tsao, MD<sup>2</sup>, and Ignacio I. Wistuba, MD<sup>1,2,†</sup>

<sup>1</sup>Department of Translational Molecular Pathology, The University of Texas MD Anderson Cancer Center, Houston, Texas.

<sup>2</sup>Department of Thoracic/Head and Neck Medical Oncology, The University of Texas MD Anderson Cancer Center, Houston, Texas.

<sup>3</sup>Department of Biostatistics, The University of Texas MD Anderson Cancer Center, Houston, Texas.

<sup>4</sup>Department of Thoracic and Cardiovascular Surgery, The University of Texas MD Anderson Cancer Center, Houston, Texas.

### Abstract

**Introduction**—Malignant pleural mesothelioma (MPM) is a deadly disease with poor prognosis and few treatment options. We characterized and elucidate the roles of *C-MYC* and *PVT1* involved in the pathogenesis of MPM.

**Methods**—We used siRNA-mediated knockdown in MPM cell lines to determine the effect of *C-MYC* and *PVT1* abrogation on MPM cells undergoing apoptosis, proliferation, and cisplatin sensitivity. We also characterized the expression of *microRNAs* (*miRNAs*) spanning the *PVT1* region in MPM cell lines. Copy number analysis was measured by quantitative PCR and fluorescence in situ hybridization.

**Results**—Copy number analysis revealed copy number gains (CNGs) in chromosomal region 8q24 in six of twelve MPM cell lines. MicroRNA analysis showed high *miR-1204* expression in MSTO-211H cell lines with 4 copies of *PVT1*. Knockdown by siRNA showed increased PARP-C levels in MSTO-211H transfected with *siPVT1* but not in cells transfected with *siC-MYC*. *C-MYC* and *PVT1* knockdown reduced cell proliferation and increased sensitivity to cisplatin. Analysis of the expression of apoptosis-related genes in the MSTO-211H cell line suggested that *C-MYC* maintains a balance between pro-apoptotic and anti-apoptotic gene expression, whereas *PVT1* and to a lesser extent *miR-1204*, upregulate pro-apoptotic genes and downregulate anti-apoptotic genes. FISH analysis of MPM tumor specimens showed a high frequency of both CNGs (11/75) and trisomy (three copies; 11/75) for the *C-MYC* locus.

---

**Corresponding Author:** Ignacio I. Wistuba, Department of Translational Molecular Pathology, Unit 0951, The University of Texas MD Anderson Cancer Center, 1515 Holcombe Blvd., Houston, TX 77030, Phone: 713-792-9866; Fax: (713) 834-6082; iiwistuba@mdanderson.org.

**Disclosure of Potential Conflicts of Interest:** No potential conflicts of interest were disclosed

**Conclusion**—Our results suggest that *C-MYC* and *PVT1* copy number gain promotes a malignant phenotype of MPM, with *C-MYC* CNG stimulating cell proliferation and *PVT1* both stimulating proliferation and inhibiting apoptosis.

### Keywords

*C-MYC*; *PVT1*; 8q24 chromosomal region; Malignant pleural mesothelioma

Malignant pleural mesothelioma (MPM) is a highly aggressive cancer with a poor prognosis<sup>1</sup>. MPM's incidence in the United States has increased in recent years, 2000–3000 people are diagnosed with the disease annually<sup>2,3</sup>. MPM predominantly affects men who have been exposed to asbestos in an occupational setting<sup>4–8</sup>. The risk of developing the disease increases with age (median age at diagnosis is 72 years; range, 45 to 85 years). MPM's three major histologic subtypes are epithelioid, biphasic, and sarcomatoid<sup>1</sup>. Epithelioid tumors are the most common and have the best prognosis of the three subtypes. However, all types are very difficult to treat and have a median overall survival duration ranging from 9 to 17 months<sup>9</sup>, with an overall 2-year survival rate of only 20%<sup>10</sup>. There is therefore a great need to identify new therapeutic targets and develop more effective therapies for patients with MPM.

A potential therapeutic target for MPM and one of the most common chromosomal amplification sites in cancer tissues is the 8q24 region which contains the genes *C-MYC* and *PVT1*<sup>11–13</sup>. *C-MYC* encodes a transcription factor that regulates the expression of multiple genes involved in cellular responses such as growth, proliferation, apoptosis, and differentiation<sup>14–16</sup>. Deregulated amplification and expression of the *MYC* locus occurs in ~30% of human cancers, including colon, prostate and breast carcinomas, and has been associated with poor prognosis<sup>11,17,18</sup>. *PVT1* is a candidate oncogene located adjacent to the *MYC* locus on chromosomal region 8q24<sup>18–20</sup>. *PVT1* has been shown to act as a non-coding RNA with many alternatively spliced isoforms<sup>12,21</sup>. The *PVT1* locus has recently been found to contain a cluster of at least six microRNAs (*miRNAs*) (*miR-1204*, *-1205*, *-1206*, *-1207-3p*, *-1207-5p*, and *-1208*) that span the *PVT1* region, adding further complexity to the locus<sup>12,21</sup>. *PVT1* copy number gains (CNGs) and *PVT1* overexpression both have been implicated in the pathophysiology of many tumors, including breast and ovarian cancers and acute myeloid leukemia<sup>19,22</sup>. Additionally, *PVT1* alteration has been shown to contribute to tumor survival and chemoresistance<sup>22,23</sup>. However, the roles that *MYC*, *PVT1*, and *miRNAs* contained in the 8q24 chromosomal region play in MPM remain unclear. We therefore sought to elucidate these roles and the specific mechanisms of action of *C-MYC* and *PVT1* involved in the pathogenesis of MPM.

In the present study, we characterized the molecular abnormalities found in the 8q24 locus in MPM cell lines and in specimens from surgically resected MPMs. Characterized the *miRNA* (*miR-1204*, *-1205*, *1206*, *-1207 3p*, *1207-5p*, and *-1208*) expression in MPM cell lines. We also determined the biological impact of siRNA-mediated *C-MYC* and *PVT1* abrogation on MPM cellular processes such as apoptosis, cell proliferation, and response to cisplatin and then determined the effect of *C-MYC*, *PVT1*, and *miR-1204* knockdown on the

expression levels of apoptosis related genes. Finally, we studied *C-MYC* and *PVT1* copy number and gene expression in MPM tumor specimens.

## MATERIALS AND METHODS

### Tumors Specimen and Cell Lines

From the tissue bank at The University of Texas MD Anderson Cancer Center, we obtained archived frozen and formalin-fixed, paraffin-embedded (FFPE) tissues for patients who had undergone surgical resection for MPM. We randomly selected 75 MPM samples of different histologic subtypes (37 epithelioid, 26 biphasic, 12 sarcomatoid) for analysis. Detailed clinical and pathologic information on the patients is presented in Supplementary Table 1. The study protocol was approved by the MD Anderson institutional review board. Of the 12 MPM cell lines used in this study, five (H2452, MET-5A, H2052, H28 and MSTO-211H) were obtained from the American Type Culture Collection (Manassas, VA) and cultured in RPMI 1640 (Cellgro Mediatech, Manassas, VA), and seven (HCT-4012, Meso, HP3, HP5, HP7, HP9 and HP10) were acquired from Dr. Harvey Pass (New York University, New York, NY) and cultured in high-glucose Dulbecco's modified Eagle's medium (DMEM) (Cellgro Mediatech, Manassas, VA). All media formulations included 10% fetal bovine serum (FBS) and antibiotics (Sigma-Aldrich, St. Louis, MO). All MPM cell lines had been tested for absence of mycoplasma using Universal Mycoplasma Detection Kit according to manufacturer's instructions (ATCC, Manassas, VA) and cells were authenticated at UTMDACC Core Facility.

### Isolation of DNA and Copy Number Profiling

DNA was extracted from cell lines using DNAzol Reagent (Life Technologies, Grand Island, NY) and whole-genome single nucleotide polymorphism (SNP) array profiling was performed using Affymetrix SNP 6.0 chips (Agilent Technologies, Santa Clara, CA) in five MPM cell lines. Copy number gains (CNGs) were identified using the SNP-Fast Adaptive States Segmentation Technique 2 algorithm in Nexus 5.1 software (BioDiscovery, Hawthorne, CA) with the significance threshold for segmentation setting at  $p < 5 \times 10^{-7}$ . CNGs were defined with log2 ratio values of 0.2, and two or more than two CNGs were defined by log2 ratio values of 0.7.

### Copy Number Analysis

We used fluorescence in situ hybridization (FISH) and real-time quantitative PCR (q-PCR) to quantify 8q24 CNGs in MPM tumor specimens. We used directly labeled fluorescent chromosomal centromeric probes (CEP 8, SpectrumGreen) for chromosome 8 and locus-specific probes (LSI) for regions 8q24.12-q13 (*C-MYC* Spectrum Orange) (Vysis, Abbott Laboratories, Chicago, IL). Fluorescence in situ hybridization (FISH) was performed according to the manufacturer's instructions. Copy number analysis was performed in 50 nuclei per tumor in at least four areas. Copy number alteration was defined as the presence of more than two gene copies per cell on average of the 50 cells. Trisomy was defined as the presence of three copy number alterations and CNG was defined the presence of at least four copies. To enrich for malignant cell content for q-PCR analysis, tumor tissues were manually microdissected for subsequent DNA extraction from FFPE tissue sections. Tumor

DNA was extracted using the Pico Pure DNA Extraction Kit (Arcturus, Life Technologies, Grand Island, NY) according to the manufacturer's instructions. DNA samples with proportions of microdissected tumor cell greater than 70% were qualified for qPCR analysis. *MYC* and *PVT1* gene copy numbers were examined by q-PCR using the comparative Ct method using the ABI 7300 real time PCR system (Applied Biosystems, Grand Island, NY). The sequences of PCR primers used to CNG was for *C-MYC*, 5'-TCAAGAGGTGCCACGTCTCC-3' and 5'-TCTTGGCAGCAGGATAGTCCTT-3' (flanking exon 3), for *PVT1*, 5'-ACAGTGATCTTCAGTGGTCTGG-3' and 5'-CGTGTGTCATTCCAGTGCAT-3' (flanking exon 2). Each PCR was carried out using Power SYBR Green PCR Master Mix (Applied Biosystems) at 50°C for 2 minutes and 95°C for 10 minutes followed by 40 cycles at 95°C for 15 seconds and 60°C for 1 minute.  $\beta$ -Actin was introduced as the endogenous reference gene, and TaqMan Control Human Genomic DNA (Applied Biosystems) was amplified as a standard control for calibration. *MYC* and *PVT1* gene copy number in normal human genomic DNA was set as 2 and copy number 4 was considered as CNG<sup>24</sup>. All sample and standard DNA reactions were set in triplicate to gauge reaction accuracy.

### Isolation of mRNA and *miRNA* Analysis

Total RNA was extracted from frozen MPM tumor specimens and cell lines using TRI Reagent (Life Technologies, Grand Island, NY). Spectrophotometric analysis using Nanodrop 1000 (Nanodrop-Thermo Fisher Scientific, Waltham, MA) was used to quantify RNA, and Agilent BioAnalyzer RNA nano-chips (Agilent Technologies, Santa Clara, CA) were used to gauge RNA quality. Affymetrix U133 Plus 2.0 gene expression arrays (Affymetrix, Santa Clara, CA) were used to determine global expression levels of genes, including *MYC* and *PVT1* in the total RNA extracted from tumor specimens. Using a High Capacity RNA-to-cDNA Kit and Taqman Gene Expression PCR Assays (Applied Biosystems, Grand Island, NY), we performed quantitative reverse transcriptase polymerase chain reaction (qRT-PCR) analysis of the RNA extracted from cell lines to quantify *MYC* and *PVT1* levels. The sequences of PCR primers used to gene expression was for *C-MYC*, 5'-CAGCTGCTTAGACGCTGGATT-3' (flanks between exon 1 and 2), and 5'-GTAGAAATACGGCTGCACCGA-3', for *PVT1*, 5'-TTACAGGCGTGTGCCACAAAGC-3', and 5'-GCCTGTAATCCCAGCACGTTGA-3' (flanks between exon 5 and 6). *GAPDH* was used as the endogenous control. TaqMan microRNA assays (Applied Biosystems, Grand Island, NY) were used to quantify the levels of *miRNAs* (*miR-1204*, *-1205*, *-1206*, *-1207-3p*, *-1207-5p*, and *-1208*) with U6 as the endogenous control. Standard PCR assays were performed on triplicate samples in standard cycling conditions using the ABI PRISM 7300 Sequence Detection System (Applied Biosystems Grand Island, NY). This process was used to yield relative expression levels using the  $2^{-C_T}$  method with the help of ABI 7300 System SDS v1.4 software (Applied Biosystems, Grand Island, NY).

### TaqMan Human Apoptosis Array

TaqMan gene expression assays were used along with the three control genes (*18S*, *ACTB*, and *GAPDH*) to detect the expression levels of the 93 apoptosis-related genes on a microfluidic 384-well array (TaqMan® Array Human Apoptosis, Applied Biosystems, Grand

Island, NY), using an Applied Biosystems 7900HT Fast Real-Time PCR System (Applied Biosystems-Life Technologies, Grand Island, NY). Fold changes of gene expression in experimental samples were quantified relative to the control samples using the equation  $2^{-(C_T)}$ . Data were analyzed using Data Assist software version 3.0 (Life Technologies) and a 2.0-fold change in gene expression was defined as the threshold for up- or down-regulation.

### MTS Assay

Cisplatin was purchased from Selleck Chemicals, Houston, TX. To determine the median half-maximal inhibitory concentration (i.e.,  $IC_{50}$ ), cells were seeded in octuplicate at a density of 2,000 per well in 96-well plates. 24 hours later, cells were treated with increasing concentrations (0 to  $30\mu\text{M}$ ) of drugs. An endpoint viability assay using MTS (3-(4,5-dimethylthiazol-2-yl)-5-(3-carboxymethoxyphenyl)-2-(4-sulfophenyl)-2H-tetrazolium, inner salt) assays (Promega, San Luis Obispo, CA) was performed after 72 hours of drug treatment.

### siRNA Transfection and Cell Proliferation Assays

Cell lines were transfected with two gene-specific siRNA duplexes for each gene (*C-MYC* and *PVT1*) and control siRNA (Ambion, Grand Island, NY) at a final concentration of 10 nmol/L using Lipofectamine RNAiMAX (Invitrogen, Grand Island, NY) according to the manufacturer's instructions. To verify the knockdown's efficiency, we collected the mRNAs and protein of transfected cells and subjected them to qRT-PCR and Western blot analysis. *miRNA* inhibitor anti-*miR-1204* was used to downregulate *miR-1204* expression in MSTO-211H MPM cell line and the *miRNA* inhibitor negative control, at a final concentration of 50 nmol/L using Lipofectamine RNAiMAX (Invitrogen, Grand Island, NY) according to the manufacturer's instructions. *miRNA* inhibition by anti-*miRNA* was assessed by TaqMan microRNA Assays with *U6* as the endogenous control (Applied Biosystems, Grand Island, NY). Proliferation assays were carried out by MTS assay according to the manufacturer's protocols (Promega, San Luis Obispo, CA). Western blot analysis was carried out using specific antibodies against C-MYC (Santa Cruz Biotechnology, Santa Cruz, CA) and the analysis cleaved poly(ADP-ribose) polymerase (PARP-cleaved; Asp214; Cell Signaling Technology, Danvers, MA) and cleaved Caspase 3 (Cleaved Casp3; Asp175; Cell Signaling Technology, Danvers, MA).

### Statistical Analysis

Data obtained from cell culture assays and from the qRT-PCR and Western blot analyses were summarized using descriptive and inferential statistics accompanied by graphs of relative expression created using the Prism software program (version 5.0; GraphPad Software, La Jolla, CA). DNA copy number analysis using Affymetrix SNP6.0 microarray chip was conducted on Nexus 5.1 software (BioDiscovery, Hawthorne, CA). Analysis clinical and demographic data for the patients whose archived tumor samples were analyzed using the chi-square, Fisher exact, Wilcoxon rank-sum, and Kruskal-Wallis tests. Overall survival (OS) and recurrence-free survival (RFS) distributions were estimated using the Kaplan-Meier method, compared between groups of patients using the log-rank test. Cox

proportional hazard models were used to calculate OS duration data and which was defined as the time from surgery to the patient's death or last contact, and for RFS duration, which was defined as the time from surgery to tumor recurrence or the patient's last contact.

## RESULTS

### 8q24 Locus amplification and *C-MYC* and *PVT1* Expression in MPM Cell Lines

We performed global SNP/copy number analysis using Affymetrix SNP 6.0 chips in four MPM cell lines (H28, MSTO-211H, H2052, and H2452) and, for comparison, in the control normal cell line HCC-4012 (a telomerase-transformed pleural mesothelial cell line). DNA copy number analysis revealed CNG of chromosomal region 8q24, which contains both the *C-MYC* and *PVT1* genes, in three of the five MPM cell lines (MSTO-211H, H2052, and H2452) relative to the control cell line (HCC-4012; Fig. 1A and 1B). In order to confirm our finding of CNG of the *C-MYC* locus in MPM cell lines, we performed FISH and q-PCR on 12 MPM cell lines. FISH analysis revealed a relatively high frequency of CNG defined as 4 copies of the *C-MYC* locus (6/12, 50%; Fig. 1C). Similarly, q-PCR analysis of genomic DNA showed a high frequency (5/12, 42%) of *C-MYC* CNG, also defined as 4 copies (Fig. 1D). We also used q-PCR to quantify CNG for the *PVT1* gene, again detecting a high frequency (5/12, 42%) of *PVT1* CNG (Fig. 1D). Interestingly, *C-MYC* and *PVT1* CNGs were always detected in the same cell lines (H2452, MET 5A, H2052, HP10, and MSTO-211H). Of these cell lines, only HP10 and MSTO-211H had amplification for *C-MYC* (>15 copies).

To determine whether *C-MYC* and *PVT1* expression levels were also elevated in MPM cell lines, we analyzed mRNA expression using qRT-PCR of both genes on 12 MPM cell lines. qRT-PCR analysis showed increased levels (i.e., 4-fold changes) of *C-MYC* gene expression in five MPM cell lines (HP3, HP7, H28, H2052, and MSTO-211H). For the *PVT1* gene, only the MSTO-211H cell line with CNG for *PVT1* showed an increased level of gene expression (4-fold change) (Fig. 1E). We did not detect increased levels of *PVT1* gene expression in the other MPM cell lines that had CNG for *PVT1*.

### *miRNA* Expression in the *PVT1* region in MPM Cell Lines

*PVT1* encodes a non-coding RNA and is a host gene for the following *miRNAs* several *miRNAs*, including: *miR-1204*, *-1205*, *-1206*, *-1207-3p*, *-1207-5p*, and *-1208*. We screened a panel of seven MPM cell lines for expression of *miR-1204*, *-1205*, *-1206*, *-1207-3p*, *-1207-5p* and *-1208* in the *PVT1* region using qRT-PCR. We detected expression of *miR-1204*, *-1205*, *-1207-5p*, and *-1208* in all seven MPM cell lines (Fig. 1F and Supplementary Table 2). We did not detect *miR-1206* or *miR-1207-3p* expression in any of the cell lines tested. Interestingly, the MSTO-211H cell line with *PVT1* CNG showed elevated expression of *miR-1204* (4 fold change) and *miR-1208* (2 fold change). Additionally, we detected a relatively high expression of *miR-1205* in HP10 (3 fold change).

## The Roles of *C-MYC* and *PVT1* in Oncogenesis

To examine the effects of abrogation of *C-MYC* and *PVT1* function in MPM cell lines, we knocked down *C-MYC* and *PVT1* in the MSTO-211H and H28 MPM cell lines using specific siRNA. Cell lines were selected for their numbers of *C-MYC* and *PVT1* CNG (>10 copies and <4 copies, respectively). In both cell lines, qRT-PCR analysis showed that *C-MYC* and *PVT1* knockdown significantly decreased mRNA expression relative to control siRNA-transfected and non-transfected cells (Fig. 2A and 2B). We first assessed the cytotoxic effects of *C-MYC* and *PVT1* knockdown on MPM cell lines by inducing apoptosis (Fig 2C and 2D). We found that *PVT1* knockdown increased PARP-cleaved and cleaved Caspase 3 expression in the MSTO-211H cell line relative to control siRNA-transfected and nontransfected cells 72 hours after transfection (Fig. 2C and Supplementary Fig 2). After transfection of si*C-MYC*, we observed a decrease, rather than an increase, in PARP-cleaved levels (Fig. 2C). We did not detect changes in PARP-cleaved levels under any treatment of the H28 cell line (Fig. 2D). Interestingly, we found that *C-MYC* knockdown by siRNA induced a decrease in *PVT1* expression in the MSTO-211H and H28 cell lines, suggesting that *C-MYC* might regulate *PVT1* expression in the MSTO-211H cell lines (Fig. 2A and B).

We additionally investigated the effect of *C-MYC* and *PVT1* knockdown by siRNA on cell proliferation. We found significant proliferation inhibition in the MSTO-211H cell line when knocked down *C-MYC* and *PVT1* (Fig. 2E), relative to the control siRNA-transfected and nontransfected cells (Fig. 2E). Proliferation was more strongly inhibited when we knocked down *PVT1* than when we knocked down *C-MYC* in the MSTO-211H cell line. Inhibition of cell proliferation was not observed in the H28 cell line when knocked down *C-MYC* and *PVT1* (Fig. 2F).

We then evaluated the effect of *C-MYC* and *PVT1* knockdown by siRNA on the MPM cell lines' sensitivity to cisplatin. Upon treatment with si*C-MYC* and si*PVT1*, the MSTO-211H cell lines were significantly more sensitive to cisplatin *in vitro* (Fig. 2G;  $p < 0.05$ ), than were the control siRNA-transfected and non-transfected cells. This increased cisplatin sensitivity was not observed in H28 cells transfected with si*C-MYC* and si*PVT1* (Fig. 2H). These findings suggest that depletion of *C-MYC* and *PVT1* significantly contributes to increases in the sensitivity of MPM cell lines with 8q24 amplification in response to cisplatin.

We also analyzed the effect on cell proliferation and cisplatin sensitivity of *miR-1204* downregulation by anti-*miR-1204* in MSTO-211H MPM cell lines. qRT-PCR showed that anti-*miR-1204* significantly decreased *miR-1204* expression relative to control cells transfected with control anti-*miRNA* and non-transfected cells (Supplementary Fig. 1A). However, we found no significant differences between cells treated with anti-*miR-1204*, control cells transfected with control anti-*miRNA*, and non-transfected cells in terms of cisplatin sensitivity (Supplementary Fig. 1B) and proliferation (Supplementary Fig. 1C). These finding suggest that changes in apoptosis and cisplatin sensitivity produced by *PVT1* are not mediated by *miR-1204*; rather, these *PVT1*-driven changes may be mediated, either individually or jointly, by other *miRNAs* spanning the *PVT1* region.

Overall, our *in vitro* analysis strongly supports our hypothesis that 8q24 amplification can contribute to different oncogenic functions in MPM cancer cells. Specifically, CNGs of *C-*

*MYC* stimulates cell proliferation, and CNGs of *PVT1* stimulates proliferation and inhibits apoptosis.

### Regulation of Apoptosis-Related Gene Expression by *C-MYC* and *PVT1*

Our *in vitro* findings demonstrate that *PVT1* knockdown increases PARP-cleaved and cleaved Caspase 3 expression in the MSTO-211H cell line. In contrast, after *C-MYC* knockdown, we observed a decreased PARP-cleaved expression. The effects of *C-MYC* and *PVT1* knockdown suggest that although both genes regulate apoptosis, they do so by alternative means. To understand how these genes are orchestrated to regulate apoptosis, we used the TaqMan Human Apoptosis Array to study the expression of 93 genes involved in apoptosis in two MPM cell lines with *C-MYC* and *PVT1* CNGs; MSTO-211H cell line transfected with si*C-MYC*, si*PVT1*, and anti-*miR-1204* and HP10 cell line transfected with si*C-MYC* and si*PVT1*.

Table 1 and supplementary Table 3 depicts changes in the expression levels of apoptosis-related genes after knockdown of *C-MYC*, *PVT1*, and *miR-1204* (2.0-fold change of expression). Knockdown of *C-MYC* in the MSTO-211H cell line reveal seven genes that were upregulated (*LTB*, *BIRC7*, *BCL2L14*, *PYCARD*, *BCL2A1*, *FASLG*, and *BIRC2*) and three genes that were downregulated (*NFKB1*, *BBC3*, and *TNFRSF21*) relative to nontransfected cells or cells transfected with scrambled siRNA (control). Of the upregulated genes, four have known apoptotic functions (*LTB*, *BCL2L14*, *PYCARD*, and *FASLG*) and the remaining three (*BIRC7*, *BCL2A1*, and *BIRC2*) have known anti-apoptotic function. Among the downregulated genes, one gene (*NFKB1*) has anti-apoptotic function and two (*BBC3* and *TNFRSF21*) have pro-apoptotic function. *PVT1* knockdown upregulated five genes (*LTB*, *BCL2L14*, *PYCAR*, *FASLG*, and *TNFRSF1B*) and downregulated six genes (*BCL2L1*, *BCL2*, *ICEBERG*, *CASP5*, *TNF*, and *BIRC8*) relative to the expression levels of nontransfected cells or cells transfected with scrambled siRNA (i.e., controls). All genes whose expression was enhanced by *PVT1* knockdown have pro-apoptotic function. Four of the downregulated genes (*BCL2L1*, *BCL2*, *ICEBERG*, and *BIRC8*) have anti-apoptotic function, whereas the other two downregulated genes (*CASP5* and *TNF*) have pro-apoptotic function. Knockdown of *C-MYC* and *PVT1* in the HP10 cell line revealed a similar tendency of genes upregulated and downregulated, but less pronounced. Interestingly, one of the most highly upregulated genes in HP10 cell line was *LTB* gene also upregulated in MSTO-211H cell line after *C-MYC* and *PVT1* knockdown.

We also investigated whether *miR-1204* downregulation using anti-*miR-1204* in the MSTO-211H cell line regulated the expression of apoptosis-related genes. *miR-1204* downregulation increased the expression of five genes (*LTB*, *BIRC7*, *BCL2L14*, *PYCAR*, and *BIRC2*) and decreased the expression of three genes (*ICEBERG*, *CASP5*, and *BIRC8*). Three of the upregulated genes (*LTB*, *BCL2L14*, and *PYCAR*) have pro-apoptotic function, whereas the other two upregulated genes (*BIRC7* and *BIRC2*) are involved in anti-apoptotic function. Two of the downregulated genes (*ICEBERG* and *BIRC8*) have known anti-apoptotic function, and the other downregulated gene (*CASP5*) has pro-apoptotic function.



We found that *C-MYC* knockdown affected the expression of several pro- and anti-apoptotic genes, thus maintaining a balance between these genes. *PVT1* knockdown appeared to upregulate pro-apoptotic genes and downregulate anti-apoptotic genes. These results accord with our observation of an apoptotic phenotype of increased PARP-cleaved expression in the MSTO-211H cell line after *PVT1* knockdown—an effect we did not observe after *C-MYC* knockdown.

### **C-MYC CNG in MPM Tumors**

To validate the *C-MYC* CNG results obtained in MPM cell lines, we determined the gene copy number of the *C-MYC* locus in MPM tumor tissue specimens by performing FISH using the *C-MYC* probe on tissue microarrays (TMAs) containing 75 MPM samples from different histologic subtypes (37 epithelioid, 26 biphasic, 12 sarcomatoid). FISH analysis of TMAs revealed a high frequency of CNGs (11/75, 15%, 4 copies) and of trisomy (11/75, 15%, three copies) in the *C-MYC* locus in the MPM tumors. Interestingly, these CNGs were seen in the biphasic (6/26, 23%) and epithelioid (5/37, 13%) histotypes but not in the sarcomatoid cases (Fig. 3A, 3B, and 3C). Trisomy was seen in biphasic (6/26, 23%), epithelioid (3/37, 8%), and sarcomatoid (2/12, 17%) histotypes. Additionally, we investigated the association between *C-MYC* CNG detected by FISH and clinicopathologic features of resected MPM tissue specimens. We did not find any correlation between *C-MYC* CNGs with clinicopathologic features. After adjustment for age, tumor size, overall survival, stage, and adjuvant therapy, multivariate analysis did not show any correlation between *C-MYC* CNGs and patient outcome ( $p > 0.75$ ).

To confirm the *C-MYC* CNG results obtained using FISH, we used q-PCR to determine gene copy numbers in 30 tumor specimens (11 with *C-MYC* FISH-detected CNG and 19 without *C-MYC* FISH-detected CNG). *C-MYC* CNGs (4 copies) were detected by q-PCR in 12 MPM specimens (10 with *C-MYC* CNG and 2 without *C-MYC* CNG detected on the FISH results; Fig. 3D). Additionally, we also used q-PCR to detect *PVT1* CNG in the same 30 tumor specimens. *PVT1* CNG was detected in 12 MPM specimens (eight with *C-MYC* CNG and three without *C-MYC* CNG based on the FISH results; Fig. 3E).

We additionally determined *C-MYC* and *PVT1* mRNA expression levels in a subset of 55 MPM tumor specimens paired with 41 normal tissues from our database using Affymetrix U133 plus 2.0 chips. We found significant differences in *C-MYC* and *PVT1* gene expression between the normal tissues and the tumor samples (Fig. 3F and 3G;  $p < 0.05$ ).

## **DISCUSSION**

Our results show that amplification of the 8q24 chromosomal region occurs frequently in MPM cell lines and tumor specimens. Our *in vitro* findings suggest that *C-MYC* and *PVT1* CNG may promote a malignant MPM phenotype. We have demonstrated that *C-MYC* and *PVT1* knockdown by siRNA both increased cisplatin sensitivity and reduced cell proliferation capabilities in MPM cell lines. Interestingly, induction of apoptosis (as assessed by PARP-C levels) was observed only after *PVT1* knockdown and not after *C-MYC* knockdown. In addition, our analysis of the expression of apoptosis-related genes revealed that *C-MYC* helps to maintain a regulatory balance between the expression of pro- and anti-

apoptotic genes, whereas *PVT1* showed a trend toward upregulating pro-apoptotic genes and downregulating anti-apoptotic genes. These findings suggest the two genes have differing functions: whereas *C-MYC* CNG stimulates proliferation and helps to decrease sensitivity to cisplatin platinum therapy, *PVT1* CNG stimulates proliferation, decreases sensitivity to platinum therapy, and suppresses apoptosis. *PVT1* CNG can also contribute to the overexpression of *miRNAs* contained within this locus; we extended our study to include one of the most highly expressed of these *miRNAs*—*miR-1204*.

The 8q24 chromosomal region is frequently amplified in many tumors. This regional amplification leads to co-amplification of the *C-MYC* and *PVT1* genes located in this region<sup>19, 25</sup>. *C-MYC* encodes a transcription factor that regulates the expression of multiple genes involved in cellular processes such as growth, apoptosis, proliferation, and differentiation<sup>15–17</sup>. Deregulated *C-MYC* expression, which has been detected in a wide variety of human tumors, promotes tumorigenesis by increasing genomic instability, induces proliferation and apoptosis, stimulates angiogenesis and migration, and promotes adaptation to a hypoxic microenvironment<sup>17</sup>. We found *C-MYC* CNG to be highly frequent in MPM cell lines and tumor specimens. However, we did not find a correlation between *C-MYC* CNG with clinicopathologic features on the one hand, and patient outcomes on the other hand. The fact that we did not find a correlation may be due to the great aggressiveness of these tumors, which makes it difficult to obtain detailed clinical, treatment and long-term follow-up data for these patients.

*C-MYC* knockdown increases cisplatin sensitivity and decreases cell proliferation in MSTO-211H cell lines. Several studies have reported that MYC-mediated transcription is involved in the regulation of multiple genes, including genes involved on regulating cell cycle progression such as cyclin dependent kinases (CDK) as *CDK1*, *CDK2*, *CDK4* and *CDK6*, among others<sup>26–29</sup>. Interestingly, we observed that *C-MYC* knockdown also induces a PARP-cleaved decrease, suggesting that *C-MYC* CNGs could induce apoptosis in MPM. How *C-MYC* regulates apoptosis is a matter of continued debate. It is accepted that *C-MYC* triggers apoptosis and that its overexpression may help to sensitize cells to undergo apoptosis<sup>30–32</sup>. It has been shown *in vitro* that the withdrawal of growth factors in cells downregulates *C-MYC*, inducing cell cycle arrest, whereas *C-MYC* overexpression rapidly induces apoptosis<sup>32</sup>. *C-MYC* regulates different target genes under specific conditions and in a tissue-specific manner to regulate apoptosis<sup>14</sup>. We have shown that *C-MYC* knockdown tends to keep a balance between up- and down-regulation of the expression of pro- and anti-apoptotic genes (Table 1).

*PVT1* is frequently co-amplified with *C-MYC* in many tumors, acts as an oncogene that non-coding RNA and a cluster of at least 6 *miRNAs* that span the *PVT1* region recently has been identified<sup>12, 21</sup>. *PVT1* has been described as an *MYC* activator<sup>33</sup> and as a downstream target of both the *C-MYC* and *N-MYC* genes<sup>34</sup>. We found that *C-MYC* knockdown downregulates *PVT1* in MSTO-211H and H28 cell lines, suggesting rather that *C-MYC* might regulate *PVT1* gene expression in MPM cell lines. Additionally, *PVT1* can regulate sensitivity to certain chemotherapeutic drugs (e.g., colleagues found that *PVT1* inactivation increased gemcitabine sensitivity in human pancreatic cancer cells, contributing to cell survival and chemoresistance)<sup>23</sup>. *PVT1* knockdown by siRNA in MSTO-211H cell lines increases

cisplatin sensitivity and PARP-cleaved levels while decreasing proliferation/viability. These findings suggest that *PVT1* can act as an oncogenic non-coding RNA and that *PVT1* depletion by siRNA induces a change in gene expression that enhances response to chemotherapy and induces apoptosis.

Additionally, by analyzing the expression of apoptosis-related genes, we demonstrated that *PVT1* knockdown upregulated genes involved in pro-apoptotic functions (*LTB*, *BCL2L14*, *PYCAR*, *FASLG*, and *TNFRSF1B*) and downregulated genes involved in anti-apoptotic functions (*BCL2L1*, *BCL2*, *ICEBERG* and *BIRC8*). It therefore appears that *PVT1* depletion favors an apoptotic phenotype. Additionally, we characterized the expression of *miRNAs* spanning the *PVT1* region in MPM cell lines, showing different expression levels of these *miRNAs* in MPM cell lines and highlighting *miR-1204* overexpression in MSTO-211H cell lines with *PVT1* CNG. We also found that *miR-1204* depletion promotes the expression of anti-apoptotic genes. This finding suggests that *PVT1* CNGs, together with the action of *miRNAs* in this region, can contribute to survival and chemoresistance in MPM.

In summary, our findings indicate that *C-MYC* and *PVT1* co-amplification is frequent in MPM. *C-MYC* and *PVT1* cooperation helps to stimulate proliferation, decrease sensitivity to platinum therapy, and reduce apoptosis. Both genes also help to regulate apoptosis-related genes, with *C-MYC* revealing a tendency to maintain a balance between pro-apoptotic and anti-apoptotic genes, whereas *PVT1* revealed a tendency to upregulate pro-apoptotic genes and downregulate anti-apoptotic genes, thereby helping to suppress apoptosis.

## Supplementary Material

Refer to Web version on PubMed Central for supplementary material.

## Acknowledgments

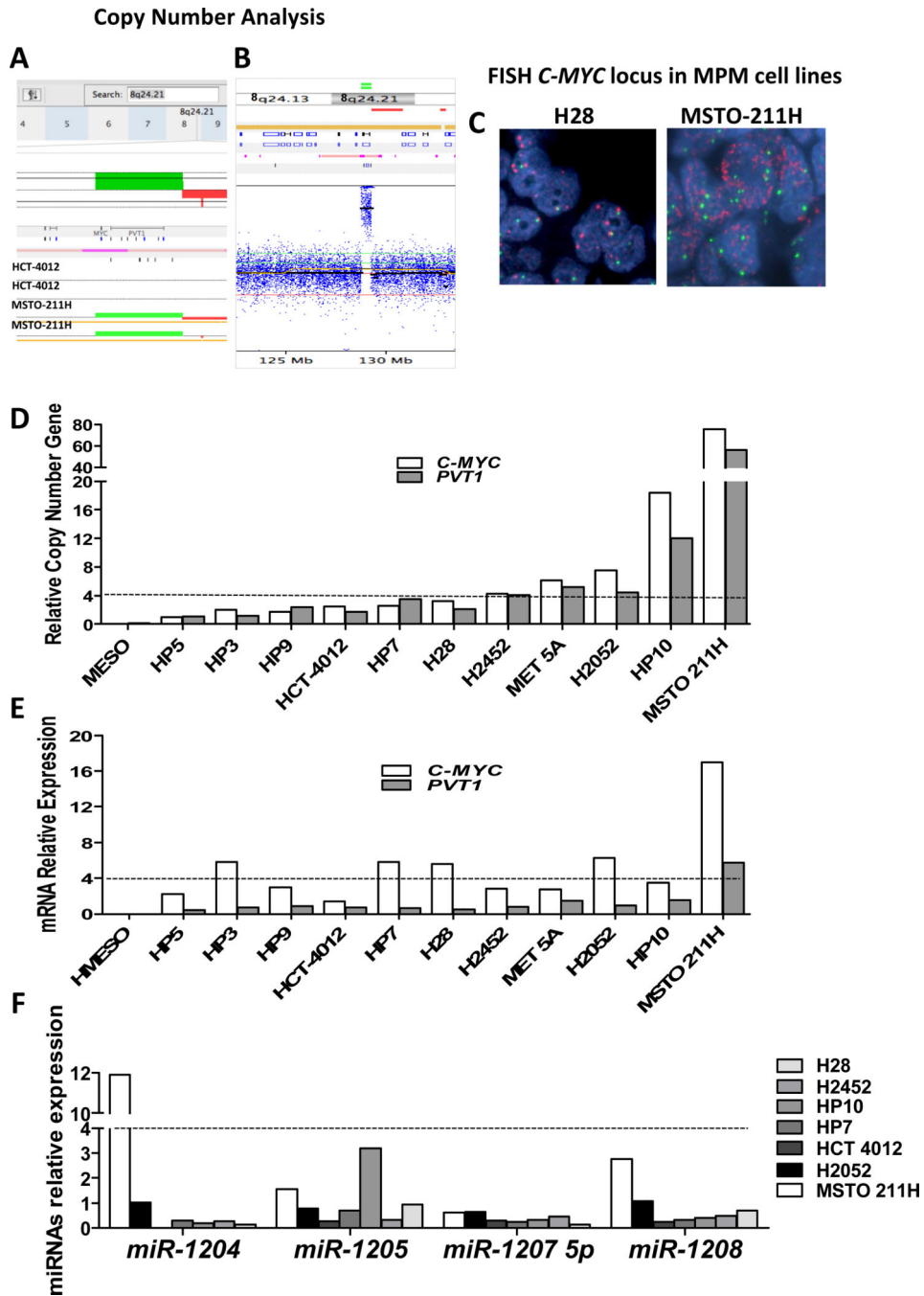
**Grant information:** This study was supported in part by grants DoD PROSPECT W81XWH-07-1-0306 and MD Anderson Cancer Center Support Grant CA016672.

## References

1. Tsao AS, Wistuba I, Roth JA, et al. Malignant pleural mesothelioma. *J Clin Oncol.* 2009; 27:2081–2090. [PubMed: 19255316]
2. Weill H, Hughes JM, Churg AM. Changing trends in US mesothelioma incidence. *Occup Environ Med.* 2004; 61:438–441. [PubMed: 15090665]
3. Price B. Analysis of current trends in United States mesothelioma incidence. *Am J Epidemiol.* 1997; 145:211–218. [PubMed: 9012593]
4. Larson T, Melnikova N, Davis SI, et al. Incidence and descriptive epidemiology of mesothelioma in the United States, 1999–2002. *Int J Occup Environ Health.* 2007; 13:398–403. [PubMed: 18085053]
5. Carbone M, Kratzke RA, Testa JR. The pathogenesis of mesothelioma. *Semin Oncol.* 2002; 29:2–17. [PubMed: 11836664]
6. Lanphear BP, Buncher CR. Latent period for malignant mesothelioma of occupational origin. *J Occup Med.* 1992; 34:718–721. [PubMed: 1494965]
7. Testa JR, Carbone M, Hirvonen A, et al. A multi-institutional study confirms the presence and expression of simian virus 40 in human malignant mesotheliomas. *Cancer Res.* 1998; 58:4505–4509. [PubMed: 9788590]

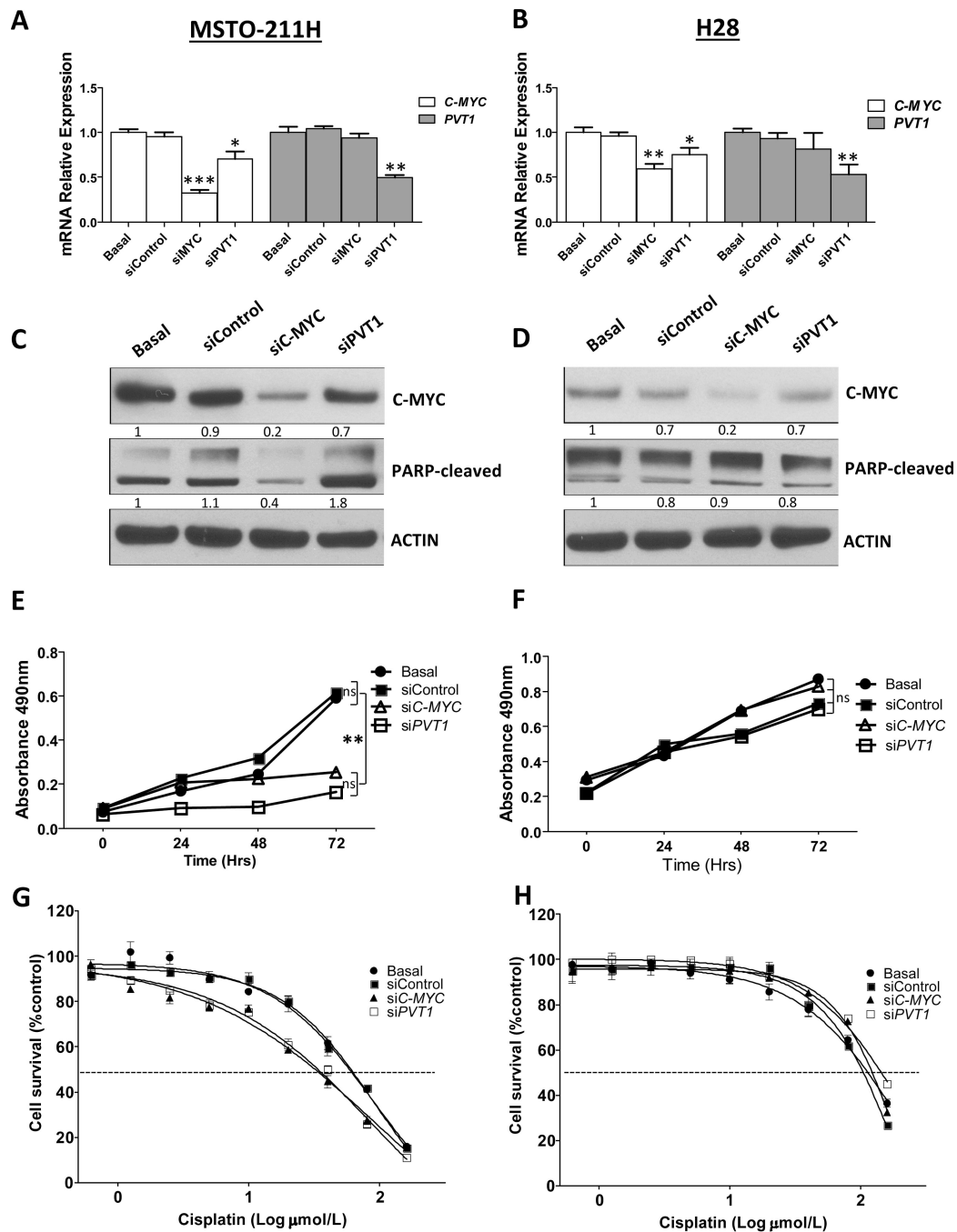
8. Carbone M, Pass HI, Rizzo P, et al. Simian virus 40-like DNA sequences in human pleural mesothelioma. *Oncogene*. 1994; 9:1781–1790. [PubMed: 8183577]
9. Zucali PA, Ceresoli GL, De Vincenzo F, et al. Advances in the biology of malignant pleural mesothelioma. *Cancer Treat Rev*. 2011; 37:543–558. [PubMed: 21288646]
10. Borasio P, Berruti A, Bille A, et al. Malignant pleural mesothelioma: clinicopathologic and survival characteristics in a consecutive series of 394 patients. *Eur J Cardiothorac Surg*. 2008; 33:307–313. [PubMed: 18164622]
11. Adhikary S, Peukert K, Karsunky H, et al. Miz1 is required for early embryonic development during gastrulation. *Mol Cell Biol*. 2003; 23:7648–7657. [PubMed: 14560010]
12. Beck-Engeser GB, Lum AM, Huppi K, et al. Pvt1-encoded microRNAs in oncogenesis. *Retrovirology*. 2008; 5:4. [PubMed: 18194563]
13. Beroukhi R, Mermel CH, Porter D, et al. The landscape of somatic copy-number alteration across human cancers. *Nature*. 2010; 463:899–905. [PubMed: 20164920]
14. Dang CV, O'Donnell KA, Zeller KI, et al. The c-Myc target gene network. *Semin Cancer Biol*. 2006; 16:253–264. [PubMed: 16904903]
15. O'Donnell KA, Yu D, Zeller KI, et al. Activation of transferrin receptor 1 by c-Myc enhances cellular proliferation and tumorigenesis. *Mol Cell Biol*. 2006; 26:2373–2386. [PubMed: 16508012]
16. Fernandez PC, Frank SR, Wang L, et al. Genomic targets of the human c-Myc protein. *Genes Dev*. 2003; 17:1115–1129. [PubMed: 12695333]
17. Dang CV, Kim JW, Gao P, et al. The interplay between MYC and HIF in cancer. *Nat Rev Cancer*. 2008; 8:51–56. [PubMed: 18046334]
18. Feo S, Di Liegro C, Jones T, et al. The DNA region around the c-myc gene and its amplification in human tumour cell lines. *Oncogene*. 1994; 9:955–961. [PubMed: 8108141]
19. Shtivelman E, Henglein B, Groitl P, et al. Identification of a human transcription unit affected by the variant chromosomal translocations 2;8 and 8;22 of Burkitt lymphoma. *Proc Natl Acad Sci U S A*. 1989; 86:3257–3260. [PubMed: 2470097]
20. Meyer KB, Maia AT, O'Reilly M, et al. A functional variant at a prostate cancer predisposition locus at 8q24 is associated with PVT1 expression. *PLoS Genet*. 2011; 7:e1002165. [PubMed: 21814516]
21. Huppi K, Volfovsky N, Runfola T, et al. The identification of microRNAs in a genomically unstable region of human chromosome 8q24. *Mol Cancer Res*. 2008; 6:212–221. [PubMed: 18314482]
22. Guan Y, Kuo WL, Stilwell JL, et al. Amplification of PVT1 contributes to the pathophysiology of ovarian and breast cancer. *Clin Cancer Res*. 2007; 13:5745–5755. [PubMed: 17908964]
23. You L, Chang D, Du HZ, et al. Genome-wide screen identifies PVT1 as a regulator of Gemcitabine sensitivity in human pancreatic cancer cells. *Biochem Biophys Res Commun*. 2011; 407:1–6. [PubMed: 21316338]
24. Yang F, Tang X, Riquelme E, et al. Increased VEGFR-2 gene copy is associated with chemoresistance and shorter survival in patients with non-small-cell lung carcinoma who receive adjuvant chemotherapy. *Cancer Res*. 2011; 71:5512–5521. [PubMed: 21724587]
25. Storlazzi CT, Fioretos T, Paulsson K, et al. Identification of a commonly amplified 4.3 Mb region with overexpression of C8FW, but not MYC in MYC-containing double minutes in myeloid malignancies. *Hum Mol Genet*. 2004; 13:1479–1485. [PubMed: 15163636]
26. Malumbres M. Physiological relevance of cell cycle kinases. *Physiol Rev*. 2011; 91:973–1007. [PubMed: 21742793]
27. Kang J, Sergio CM, Sutherland RL, et al. Targeting cyclin-dependent kinase 1 (CDK1) but not CDK4/6 or CDK2 is selectively lethal to MYC-dependent human breast cancer cells. *BMC Cancer*. 2014; 14:32. [PubMed: 24444383]
28. Prall OW, Rogan EM, Musgrove EA, et al. c-Myc or cyclin D1 mimics estrogen effects on cyclin E-Cdk2 activation and cell cycle reentry. *Mol Cell Biol*. 1998; 18:4499–4508. [PubMed: 9671459]
29. Mateyak MK, Obaya AJ, Sedivy JM. c-Myc regulates cyclin D-Cdk4 and -Cdk6 activity but affects cell cycle progression at multiple independent points. *Mol Cell Biol*. 1999; 19:4672–4683. [PubMed: 10373516]

30. Askew DS, Ashmun RA, Simmons BC, et al. Constitutive c-myc expression in an IL-3-dependent myeloid cell line suppresses cell cycle arrest and accelerates apoptosis. *Oncogene*. 1991; 6:1915–1922. [PubMed: 1923514]
31. Wyllie AH, Arends MJ, Morris RG, et al. The apoptosis endonuclease and its regulation. *Semin Immunol*. 1992; 4:389–397. [PubMed: 1337478]
32. Evan GI, Wyllie AH, Gilbert CS, et al. Induction of apoptosis in fibroblasts by c-myc protein. *Cell*. 1992; 69:119–128. [PubMed: 1555236]
33. Graham M, Adams JM. Chromosome 8 breakpoint far 3' of the c-myc oncogene in a Burkitt's lymphoma 2;8 variant translocation is equivalent to the murine pvt-1 locus. *EMBO J*. 1986; 5:2845–2851. [PubMed: 3024964]
34. Carramusa L, Contino F, Ferro A, et al. The PVT-1 oncogene is a Myc protein target that is overexpressed in transformed cells. *J Cell Physiol*. 2007; 213:511–518. [PubMed: 17503467]



**Figure 1.** *C-MYC* locus amplification is observed in malignant pleural mesothelioma (MPM) cell lines but not in normal mesothelial cell lines. **A**, SNP/Copy number analysis by Nexus 5.1 software showed amplification (represented as green bars) of chromosomal region 8q24.21, which contains the oncogene *C-MYC*. Duplicate samples of MPM cell line MSTO-211H were compared to normal cell line HCC-4012. **B**, Copy number analysis by Nexus 5.1 software showed *C-MYC* locus amplification in a representative sample of the MSTO-211H cell line. **C**, Representative examples of *C-MYC* copy number examined by FISH in MPM

cell lines. (a) An H28 specimen shows no copy number gain (CNG). (b) An MSTO-211H specimen shows CNG. Red signals represent the *C-MYC* gene probe, whereas green signals represent the internal control probe (magnification 1,000×). *D*, q-PCR analysis of *C-MYC* and *PVT1* CNG in MPM cell lines. *E*, Relative expression of *C-MYC* and *PVT1* mRNA by qRT-PCR in MPM cell lines showed increased levels (i.e., 4-fold changes) of *C-MYC* gene expression in five MPM cell lines (HP3, HP7, H28, H2052, and MSTO-211H) and only the MSTO-211H cell line showed an increased level of *PVT1* gene expression (4-fold change). *F*, Relative expression of *miRNAs* by qRT-PCR in MPM cell lines showed expression of *miR-1204*, *-1205*, *-1207-5p*, and *-1208* in all seven MPM cell lines expression of *miR-1204*, *-1205*, *-1207-5p*, and *-1208* in all seven MPM cell lines and not detect *miR-1206* or *miR-1207-3p* expression in any of the cell lines tested.

**Figure 2.**

Knockdown of *C-MYC* and *PVT1* by siRNA decreased expression of *C-MYC* and *PVT1*, increased sensitivity to cisplatin, and reduced cell proliferation in malignant plural mesothelioma (MPM) cell lines. *A*, qRT-PCR analysis of *C-MYC* and *PVT1* expression showed decreased *C-MYC* and *PVT1* expression after knockdown of *C-MYC* and *PVT1* by siRNAs in the MSTO-211H cell line. *B*, H28 MPM cell lines showed decreased *C-MYC* and *PVT1* expression after knockdown of *C-MYC* and *PVT1* by siRNAs. \*\*\* $p < 0.001$ , \*\* $p < 0.01$ , \* $p < 0.05$ . *C*, Western blot analysis of C-MYC and PARP-C expression after



knockdown of *C-MYC* and *PVT1* in MSTO-211H cell lines showed decreased expression of C-MYC and increased PARP-C levels. *D*, Knockdown of *C-MYC* and *PVT1* by siRNAs in H28 MPM cell lines showed decreased expression of C-MYC, and not detect changes in PARP-C levels when knocked down C-MYC and PVT1 in the H28 cell line *E*, Knockdown of *C-MYC* and *PVT1* significantly reduced cell proliferation in MSTO-211H.  $**p < 0.01$ . *F*, However, proliferation was not reduced in H28 MPM cell lines. *G*, Knockdown of *C-MYC* and *PVT1* by siRNA caused a 1.9-fold ( $p < 0.05$ ) and 1.7-fold ( $p < 0.05$ ) decrease in the cisplatin IC<sub>50</sub> in MSTO-211H cell lines. *H*, However, knockdown did not cause cisplatin IC<sub>50</sub> to decrease in H28 MPM cell lines. MPM cells subjected to gene-specific siRNA experiments were compared with control siRNA-transfected and nontransfected cells.

FISH *C-MYC* Locus in MPM Tumor

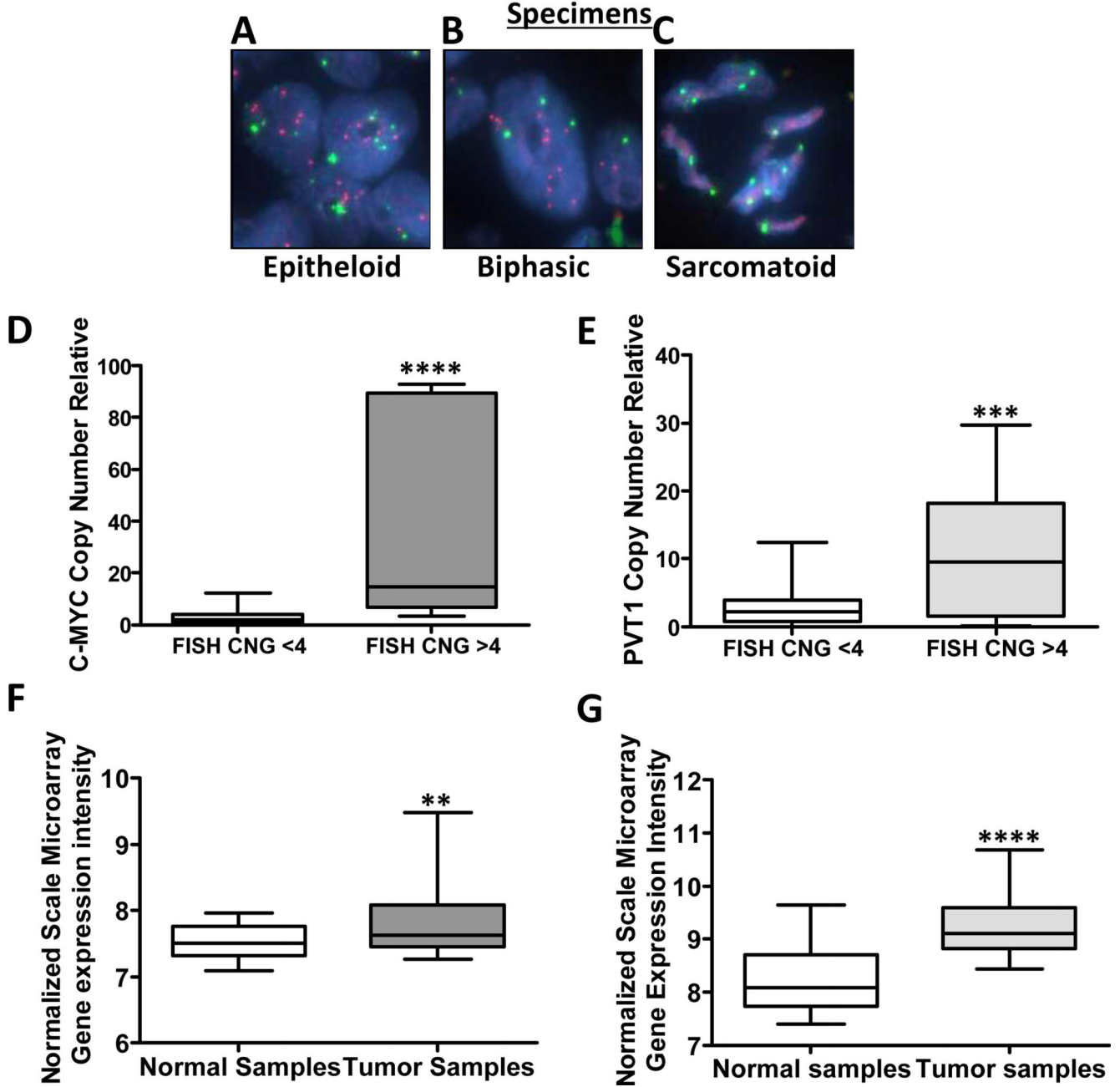


**Figure 3.** Malignant plural mesothelioma (MPM) tumor tissue specimens show *C-MYC* and *PVT1* locus-specific copy number gain (CNG) and high expression of *C-MYC* and *PVT1*. Representative examples of *C-MYC* CNG examined by Fluorescence in situ hybridization (FISH) in MPM tissue specimens show high frequency of CNGs. FISH analysis shows, *A*, CNGs in epithelioid MPM. *B*, CNGs in biphasic MPM. *C*, no CNG in sarcomatoid MPM. Red signals represent the *C-MYC* gene probe, whereas and green signals represent the internal control probe (magnification 1,000×). Real time quantitative PCR (q-PCR) analysis

of CNG of *C-MYC* and *PVT1* in MPM tumor specimens by compared with CNG by FISH shows a correlation between both approaches. *D*, The box plots depict relative CNG of *C-MYC* revealed by q-PCR in 11 MPM tumor cell lines with *C-MYC* CNG as established by FISH and 19 MPM tumor cell lines without *C-MYC* CNG as established by FISH. \*\*\*\*  $p < 0.0001$ . *E*, The box plots depict relative CNG of *PVT1* by q-PCR in 11 MPM tumor cell lines with *C-MYC* CNG as established by FISH and 19 MPM tumor cell lines without *C-MYC* CNG as established by FISH. \*\*\*  $p < 0.001$ . Normalized mRNA expression analysis *F*, *C-MYC* and *G*, *PVT1* transcript using Affymetrix U133 plus 2.0 chips in MPM tumor specimens compared with normal samples. \*\*\*\*  $p < 0.0001$ , \*\*  $p < 0.01$ .

**Table 1**  
Gene Expression of Apoptosis-related Genes After Knockdown *C-MYC*, *PVT1* and *miR-1204* in MSTO-211H Cell Lines

Gene Name	Fold Change				Gene Description	Function
	siC-MYC	siPVT1	Anti-miR-1204			
<b>Genes upregulated</b>						
<i>LTB</i>	<b>17.56</b>	<b>7.31</b>	<b>5.25</b>		Lymphotoxin beta	Pro-apoptotic
<i>BIRC7</i>	<b>9.96</b>	-1.61	<b>8.83</b>		Baculoviral IAP repeat-containing protein 7	Anti-apoptotic
<i>BCL2L14</i>	<b>9.43</b>	<b>4.35</b>	<b>6.57</b>		BCL2 like protein 14	Pro-apoptotic
<i>PYCARD</i>	<b>9.59</b>	<b>-4.06</b>	<b>9.92</b>		PYD and card domain-containing protein	Pro-apoptotic
<i>BCL2A1</i>	<b>3.79</b>	-1.23	1.41		BCL2-related protein A1	Anti-apoptotic
<i>FASLG</i>	<b>3.29</b>	<b>3.03</b>	1.27		FAS ligand	Pro-apoptotic
<i>BIRC2</i>	<b>2.93</b>	1.66	<b>2.22</b>		Baculoviral IAP repeat-containing protein 2	Anti-apoptotic
<i>TNFRSF1B</i>	0.89	<b>2.12</b>	1.50		Tumor necrosis factor receptor superfamily member 1B	Pro-apoptotic
<b>Genes downregulated</b>						
<i>NFKB1</i>	<b>-2.15</b>	1.49	1.01		Nuclear factor NF-kappa-B p105 subunit	Anti-apoptotic
<i>BBC3</i>	<b>-2.20</b>	-1.17	1.01		BCL2 binding component 3	Pro-apoptotic
<i>TNFRSF21</i>	<b>-2.50</b>	1.21	-1.75		Tumor necrosis factor receptor superfamily member 21	Pro-apoptotic
<i>BCL2L1</i>	1.11	<b>-2.02</b>	-1.35		BCL2 like 1	Anti-apoptotic
<i>BCL2</i>	-1.47	<b>-2.13</b>	-1.05		B-cell lymphoma 2	Anti-apoptotic
<i>ICEBERG</i>	1.26	<b>-6.95</b>	<b>-5.31</b>		Caspase 1 inhibitor	Anti-apoptotic
<i>CASP5</i>	-1.08	<b>-9.52</b>	<b>-2.47</b>		Caspase 5, apoptosis related cysteine protease	Pro-apoptotic
<i>TNF</i>	-1.43	<b>-11.48</b>	-1.62		Tumor necrosis factor	Pro-apoptotic
<i>BIRC8</i>	1.10	<b>-42.69</b>	<b>-2.47</b>		Baculoviral IAP repeat-containing protein 8	Anti-apoptotic

Bold, 2.0-fold change of expression,  $p < 0.05$